Available on CMS information server **CMS CR 2004/046**

# CMS Conference Report

**28 September 2004**

# The CMS tracker

M. Weber

*CERN, Geneva, Switzerland*

***CMS collaboration***

**Abstract**

The tracker for the CMS detector at the LHC experiment will provide the possibility to both tag and reconstruct in detail $b$-jets and $b$-hadrons inside those jets. 15.148 silicon strip detectors and a pixel vertexing system allow secondary vertices to be found over the full CMS acceptance. This is necessary to study $B$-hadron physics including CP-violation, $B_s$ oscillations and rare $B$-decays right after the start of the experiment.

After a more general description of the detector layout, expected results in terms of reconstruction capability with a special attention to vertexing and heavy flavor tagging are given.

Presented at *BEACH04*, Chicago, July 2nd, 2004

# 1 Introduction

The Compact Muon Solenoid (CMS) detector is currently under construction and will be installed in the tunnel of the LHC collider at CERN, near Geneva. The LHC will provide proton on proton beams (7 TeV each) with 40 MHz collision rate. A luminosity of $10^{34}\,\mathrm{cm}^{-2}\mathrm{s}^{-1}$ will produce on average 19 collisions in one single bunch crossing for nominal LHC operation [1]. This enables the CMS physicists to explore new regions of physical interest, conducting precision measurements and searches for new physics at the same time. CMS is one of the two general purpose detectors with a broad physics programme.

The CMS detector consists of a precise muon spectrometer with a standalone resolution of $\delta p_\perp/p_\perp$=8-15% at 10 GeV, a sampling brass hadron calorimeter, an electromagnetic lead-tungstate calorimeter with $\delta E/E$<1% for $E > 30\,\mathrm{GeV}$, a superconducting coil that provides a solenoidal 4 T magnetic field for momentum measurements, and a full silicon tracker [2, 3].

# 2 The tracker layout

An overview of the CMS tracker layout is given in figure 1. The tracker is subdivided into four silicon strip subdetectors, namely the Tracker Outer Barrel (TOB), the Tracker Inner Barrel (TIB), the Tracker Inner Disk (TID), the Tracker Endcap (TEC), and two silicon pixel subdetectors, the pixel barrel and the pixel disks. All active components are housed in a cylindrical volume with a length of 5.4 m and a diameter of 2.4 m.

Figure 1: $r$-$z$ cut through one quarter of the CMS tracker. The black dot shows the collision point, the numbers on the top and on the right show the pseudorapidity $\eta$ coverage of the tracker.

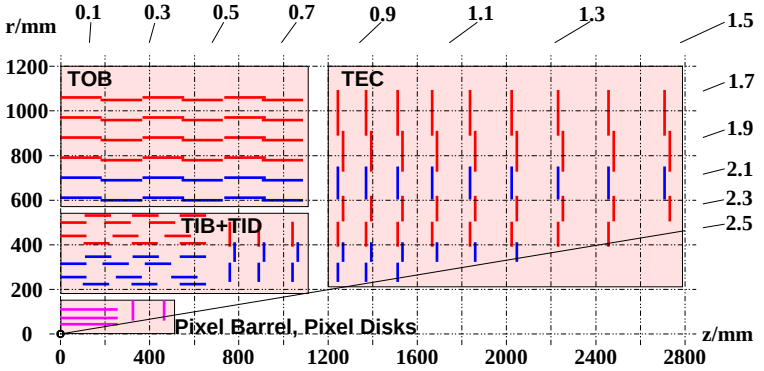


To protect the silicon detectors from thermal runaway due to increased leakage current from radiation damage in the hostile LHC environment, the full silicon tracker needs to be operated at $\approx -10°$C and thus in a dry environment for years. An active thermal shield placed outside of the tracker volume provides isolation, and a cooling system extracts the heat from the 60 kW power dissipation generated by the front-end electronics.

## 2.1 The Pixel Detector

The pixel detector is housed in a cylindrical volume of 1 m length and 30 cm diameter centered around the interaction point. It consists of $66 \cdot 10^6$ pixels of 100 µm($r\phi$) × 150 µm($z$), distributed over three barrel layers and two endcap disks in the final configuration. The barrel layers are placed at radii $r = 4.4\,\mathrm{cm}$, 7.3 cm and 10.2 cm and consist of 768 pixel modules.

Figure 2: Three layer pixel detector layout.

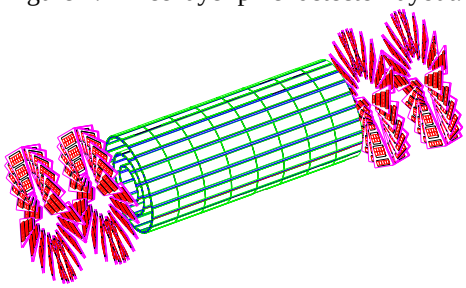

The endcap disks extend from $r = 6\,\mathrm{cm}$ to $r = 15\,\mathrm{cm}$ and consist of 672 pixel modules. They are assembled in a turbine wheel like geometry on blades with a rotation of 20° to make use of the Lorentz angle. The high Lorentz angle $\alpha_L \approx 23°$ increases the electron cloud width in the silicon for perpendicular incident particles and thus generates charge sharing between adjacent pixels. With analogue signal interpolation, a hit resolution of 10 µm($r\phi$) × 20 µm($z$) can be achieved.

The pixel module layout is as follows: a silicon baseplate is used to support the readout chips, which are bump-bonded to the silicon sensor. A high density interconnect card interfaces the readout chips to a driver chip and a capton cable. The readout chip is manufactured in a radiation hard IBM 0.25 µm process. The pixel modules consist of 16 readout chips in the barrel and 2–10 readout chips depending on the radius in the blades.

The efficiency to find three pixel hits on a track is $\epsilon_3 > 90\%$ for $|\eta| < 2.2$.

Figure 3: $p_\perp$ and impact parameter resolution (in the $r\phi$ plane and in $z$) for 1,10,100 GeV single muons as a function of the pseudorapidity $\eta$.

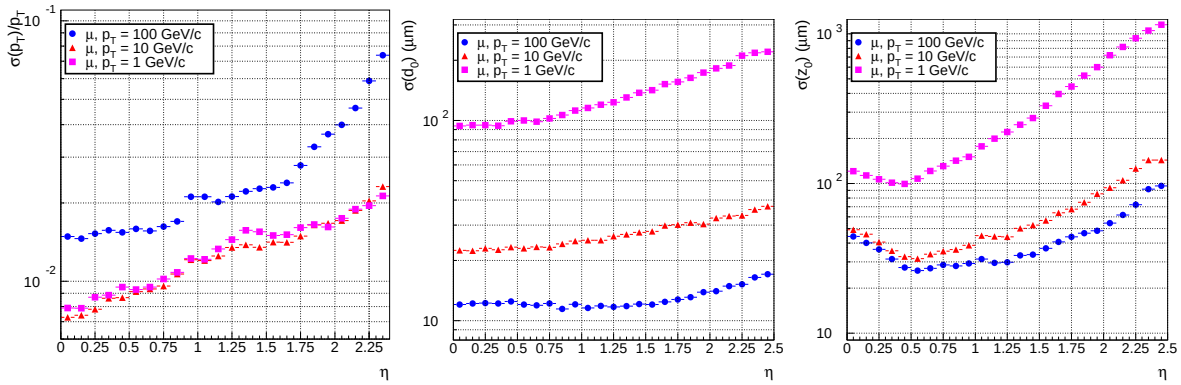


## 2.2 The Silicon Strip Tracker

The Silicon Strip Tracker consists of 15.148 silicon strip modules with a pitch from 80–205 $\mu$m distributed over 10 barrel layers (4 TIB, 6 TOB) and 3 TID and 9 TEC disks (cf. figure 1). Layers 1 and 2 (counted from the inside) from TIB and TOB as well as TID rings 1 and 2 and TEC rings 1, 2 and 5 have back-to-back mounted modules with 100 mrad tilt, providing a stereo coordinate measurement (both $r\phi$ and $z$). Detectors of TIB, TID and the four innermost TEC rings are made of 300 $\mu$m thick sensors. The TOB and the three outermost rings of TEC consist of two sensors bonded together of 500 $\mu$m thickness.

The readout hybrid used is a four-layer polyimide hybrid that is glued to a ceramic stabiliser. It contains, depending on the number of channels, four (or six) Analouge Pipeline Voltage (APV) readout chips, fabricated in an intrinsically radiation hard 0.25 $\mu$m CMOS process. Each APV features a 128 channel, 192 beam crossings deep analogue memory. Physics data are transferred via linear laser drivers and optical fibres to off-detector digitizers. The in-detector electronics can be controlled via an optical link that implements a token-ring like protocol.

The readout hybrid is mounted on a carbon fiber frame with high voltage polyimide bias circuits, and bonded to the silicon sensors.

# 3 Tracker performance

Figure 3 shows the transverse momentum resolution $\delta p_\perp / p_\perp$ as well as the impact parameter resolution in the $r\phi$ and $z$ plane for single muons with a $p_\perp$ of 1,10,100 GeV as a function of the pseudorapidity $\eta$. For $|\eta| < 2$ and $p_\perp 10..100$ GeV, the momentum resolution is below 4%, the impact parameter resolution better than 30 $\mu$m in $r\phi$ and better than 100 $\mu$m in $z$. Track reconstruction efficiencies (for $|\eta| < 2$) for single muons are larger than 95%, 85% for single pions and around 80% for pions in jets. Whereas the efficiency varies only slightly for $|\eta| < 2$, the $p_\perp$ resolution is deteriorating due to the material budget and additionally loss of lever arm for $|\eta| > 1.6$. The radiation length in the tracker increases from $X/X_0 \approx 0.4$ for $\eta = 0$ to $X/X_0 \approx 1$ for $|\eta| \approx 1.6$.

## 3.1 Vertex finding and vertex fitting

The hard interaction primary vertex can be disentangled from those of pileup events with an algorithm that uses only the pixel detector. With this algorithm, the vertex finding efficiency is larger than 95%, and the fraction of incorrect assignment is less than 10% (with the notable exception of $H \rightarrow \gamma\gamma$).

Since the publication of the DAQ and Trigger TDR [4], a variety of new algorithms for secondary vertex fitting has been implemented in the ORCA [5] framework: linear least squares, trimmed and adaptive [6], gaussian sum and the CDF $d_0 - \phi$ [7] algorithm.

The choice of algorithm can significantly improve vertex finding efficiency and vertex resolution; as an example the adaptive vertex fitter is discussed. A distance function $F$ that can be described as a sum of weighted radii $r_i$

$$F = \sum_1^N w_i r_i, \qquad r_i = (\vec{x_V} - \vec{x_i})^T \, C \, (\vec{x_V} - \vec{x_i}) \tag{1}$$

Figure 3: Comparison of the residuals for the linear (broken line) and adaptive vertex fitter (solid line) for a benchmark scenario obtained with a simulation.

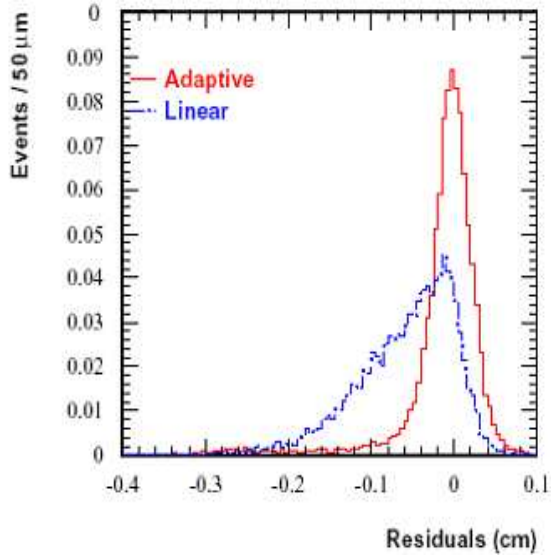


Figure 4: $b$-tagging efficiency for the track counting method as a function of the mistagging rate for $u$-jets and for different $\eta$ regions.

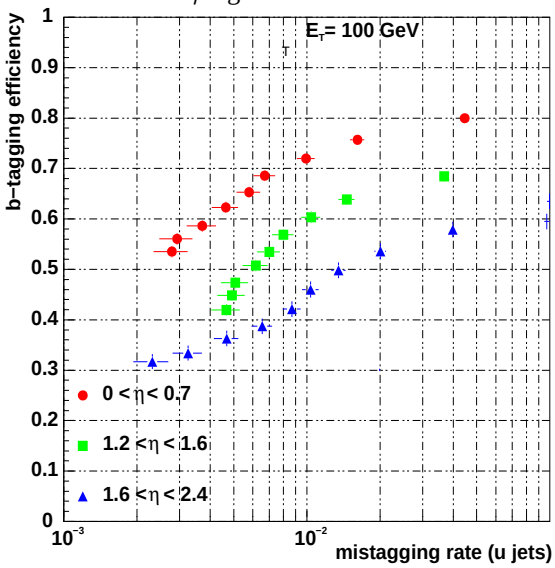


with covariance matrix $C$ is minimized, where $\vec{x_V}$ and $\vec{x_i}$ are the fitted vertex and measured track position, respectively. The advantage of this algorightm is the choice of weights $w_i$: in a trimmed algorithm, tracks either belong ($w_i = 1$) or do not belong ($w_i = 0$) to the vertex. In the adaptive vertex fitter, the weights are chosen to follow a Bose-Einstein distribution

$$w_i = \left(1 + \exp\left(\frac{r_i^2 - r_{\text{cutoff}}^2}{2T}\right)\right)^{-1}, \tag{2}$$

downweighting far tracks instead of cutting them away. The soft track cutoff parameter $r_{\text{cutoff}}$ is fixed during the minimization process, whereas the temperature $T$ is decreased in each step ("annealing") and finally reaches zero. This algorithm is more robust against mis-measured tracks and additionally the distribution of the residuals is smaller and contains less tails compared to the linear vertex fitter (cf. figure 3).

### 3.2 Tagging of *b*-jets

Several algorithms for tagging $b$-jets have already been studied in detail [8]: the track counting method, the jet probability method and the $d_0 - \phi$ algorithm. Currently work is going on to improve secondary $b$ vertex fitting and soft-lepton tagging. As an example, the simple track counting method is discussed here.

The track counting method is based on a signed three-dimensional impact parameter. It relies on an excellent track resolution (cf. figure 3).

The track counting method requires at least two tracks with an impact parameter significance exceeding a given threshold. Figure 4 shows the $b$-tagging efficiency for jets with $E_\perp = 100\,\text{GeV}$ and for different pseudorapidity regions as a function of the mistagging rate for $u$-jets. The impact parameter significance ranges from 0.5 to 4.5. An efficiency of 72% can be reached for the central CMS region ($|\eta| < 0.7$) with three pixel hits at a benchmark 1% mistagging rate for $u$-jets.

Results of the track counting method have been compared to those of the jet probability and $d_0 - \phi$ method, and similar results have been obtained.

## 4 Acknowledgements

I want to express my gratitude to CERN for the award of my fellowship, to the CMS collaboration as my hosting experiment, to my colleagues for the encouraging and fruitful collaboration, and to the conference committee for giving me the possibility to talk in such a stimulating atmosphere.

# References


[1] CERN-2004-003, 4 June 2004, Vol 1 ’The LHC Main Ring’

[2] CERN/LHCC 98-6, 15 April 1998, ’The Tracker Project Technical Design Report’

[3] CERN/LHCC 2000-016, 21 February 2000, ’Addendum to the CMS Tracker TDR’

[4] CERN/LHCC 2002-26, 15 December 2002, Vol 2 ’The Trigger and Data acquisition project’

[5] Comp. Phys. Comm., 140 (2001), p. 31, ’CMS Software Architecture’

[6] Comp. Phys. Comm. 71 (1992), p. 77 ’Track Finding With Deformable Templates: The Elastic Arms Approach’
Comp. Phys. Comm. 120 (1999), p. 197

[7] F. Abe *et al.* [The CDF collaboration], Phys. Rev. D50 (1994), p. 2966

[8] CMS Note 2002/046, 26 November 2002, ’Lifetime based $b$-tagging with CMS’